INSTITUTE FOR FUSION STUDIES

DE-FG03-96ER-54346-771 IFSR #771

Critical Nonlinear Phenomena for Kinetic Instabilities Near Threshold

B.N. BREIZMAN,[1] H.L. BERK,[1] M.S. PEKKER,[1] F. PORCELLI,[2] G.V. STUPAKOV,[3] and K.L. WONG[4]

[1] *Institute for Fusion Studies, The University of Texas at Austin Austin, Texas 78712 USA*
[2] *Dipartimento di Energetica, Politecnico di Torino, Torino 10129, Italy*
[3] *Stanford Linear Accelerator Center, Stanford University, Stanford, CA 94309 USA*
[4] *Princeton Plasma Physics Laboratory, Princeton University, Princeton, New Jersey 08543 USA*

December 1996

THE UNIVERSITY OF TEXAS

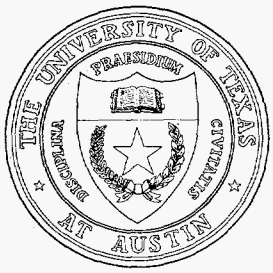

AUSTIN

DISCLAIMER

Critical Nonlinear Phenomena for Kinetic Instabilities Near Threshold

B.N. Breizman[1], H.L. Berk[1], M.S. Pekker[1],
F. Porcelli[2], G.V. Stupakov[3], and K.L. Wong[4]

[1] Institute for Fusion Studies, The University of Texas at Austin, Austin, Texas 78712 USA

[2] Dipartimento di Energetica, Politecnico di Torino, Torino 10129, Italy

[3] Stanford Linear Accelerator Center, Stanford University, Stanford, CA 94309 USA

[4] Princeton Plasma Physics Laboratory, Princeton University, Princeton, New Jersey 08543 USA

Abstract

A universal integral equation has been derived and solved for the nonlinear evolution of collective modes driven by kinetic wave particle resonances just above the threshold for instability. The dominant nonlinearity stems from the dynamics of resonant particles which can be treated perturbatively near the marginal state of the system. With a resonant particle source and classical relaxation processes included, the new equation allows the determination of conditions for a soft nonlinear regime, where the saturation level is proportional to the increment above threshold, or a hard nonlinear regime, where the saturation level is independent of the closeness to threshold. It has been found, both analytically and numerically, that in the hard regime the system exhibits explosive behavior and rapid oscillations of the mode amplitude. When the kinetic response is a requirement for the existence of the mode, this explosive behavior is accompanied by frequency chirping. The universality of the approach suggests that the theory applies to many types of resonant particle driven instabilities, and several specific cases, viz. energetic particle driven Alfvén wave excitation, the fishbone oscillation, and a collective mode in particle accelerators, are discussed.

I. Introduction

A fundamental problem in plasma physics is the evolution of kinetic instabilities driven by resonant particles.[1] Surprisingly, the nonlinear treatment of this problem has not been comprehensive and recently new insight has been obtained[2] for understanding the behavior of the system when the kinetic response of the particles can be treated as a perturbation to the linear mode. It is the purpose of this paper to generalize the earlier developed theory to problems where the kinetic response is not necessarily a perturbation to the mode and to point out that the method of analysis is applicable to a wide range of physical problems in plasma physics as well as in other areas.

One common description for the self-consistent evolution of particles and waves is quasi-linear theory,[3,4] a perturbative approach that involves many overlapped wave-particle resonances as a basis for diffusive particle transport in phase space. When resonances do not overlap global transport is strongly suppressed. Instead, as the mode grows, most of the particles respond adiabatically to the wave, and only a small selected group of resonant particles will mix and cause local flattening of the distribution function in phase space within or near the separatrices formed by the waves.

The dynamics of this process has been described by Mazitov[5] and O'Neil.[6] If the energetic particles are perturbative, and background damping is negligible, the unstable mode will grow until the bounce frequency of the resonant particles trapped in the wave, $\omega_b \sim A^{1/2}$ (with A the amplitude of the wave), reaches a level comparable to the linear growth rate.[7] The most common example is the bump-on-tail instability problem. This saturation mechanism has also been noted for other similar problems[8] and has been observed in computer simulations.[9-13] When sources and sinks are present, either higher steady state levels of saturation are obtained with relatively strong sources or periodic pulsations arise with ω_b

of order the growth rate.[8,12]

More recently, the nonlinear dynamics of a system near an instability threshold was studied when there is linear dissipation from background plasma present, and the energetic particle drive for instability gives a growth rate that just exceeds the damping rate.[2] It was shown that the dynamics is dominated by the resonant particles, and that a low level saturation occurs when the resonant particles are sufficiently collisional. However, as the collisionless limit is approached, the saturated state becomes unstable and the mode tends to grow explosively. Within the context of the perturbation theory the mode reaches an arbitrarily large amplitude in a finite time. The actual limit of applicability of this explosive solution is when the bounce frequency of the trapped particles approaches the growth rate in absence of dissipation, independent of the closeness to marginal stability. Then to within a numerical constant the saturation level near threshold is the same as when dissipation is very small.

A further generalization of this threshold analysis method is to treat nonperturbative waves, i.e., modes whose very existence requires the kinetic response of the particles. A well-known example of this is the onset of instability due to a smooth double-humped distribution.[14] Attempts have been made to understand the dynamics near threshold[15] but controversy still exists as to the validity of the solution.[16]

Unlike the work on the evolution of the double humped instability, our analysis addresses problems that involve either an additional linear dissipation from the background plasma, or higher dimensionality when the resonance lines or surfaces give both positive and negative dissipation, balanced at the instability threshold. Ironically, the classic double humped problem does not fall into this category, but there are host of other problems that do. Some examples include fishbone oscillations,[17,18] beam toroidal Alfvén eigenmodes,[19,20] hot electron interchange modes,[21] and collective modes in particle accelerators.[22] Experimentally, such modes often exhibit frequency chirping: their frequency changes in time. This change of

the mode frequency, which has not had a satisfactory theoretical explanation, appears as a natural feature in our theory.

The structure of the paper is as follows: In Sec. 2 we extend the derivation of Ref. 2 to obtain a universal nonlinear equation for a weakly unstable mode driven by resonant particles, that is applicable even to nonperturbative modes. Section 3 presents an analysis of various nonlinear scenarios described by the universal equation. Section 4 deals with possible applications of the theory and discusses correlations with several experiments.

II. Basic Equations

Near the threshold of linear instability, the evolution of the unstable mode can generally be analyzed within the assumption of a weak nonlinearity. In this limit, the perturbed current $\mathbf{J}$ that enters Maxwell's equations is a sum of $\mathbf{J}_L$, a part that is a linear functional of the mode electric field $\mathbf{E}$, and $\mathbf{J}_{NL}$, a nonlinear current whose functional dependence on $\mathbf{E}$ is calculated with a perturbation technique. Further, in this paper we assume that $\mathbf{J}_{NL}$ arises solely from resonant particles, and we neglect the other contributions to $\mathbf{J}_{NL}$ which are smaller in the range of validity of our calculations. When we use the Fourier transformed Maxwell's equations, we find

$$\int d\mathbf{r}' \mathbf{g}(\mathbf{r}, \mathbf{r}', \omega, \alpha) \cdot \mathbf{E}(\mathbf{r}', \omega) = \mathbf{J}_{NL} \tag{1}$$

where the matrix $\mathbf{g}(\mathbf{r}, \mathbf{r}', \omega, \alpha)$ includes the contribution from $\mathbf{J}_L$ and α is a parameter that measures closeness to the instability threshold. The linear theory yields the homogeneous equation

$$\int d\mathbf{r}' \mathbf{g}(\mathbf{r}, \mathbf{r}', \omega, \alpha) \cdot \mathbf{e}(\mathbf{r}', \omega) = 0.$$

At the threshold, $\alpha \equiv \alpha_{cr}$, this equation has a real eigenvalue $\omega = \omega_0$ and a nontrivial eigenvector $\mathbf{e}(\mathbf{r}, \omega_0)$ which is determined up to an arbitrary constant. Also, there exists an

adjoint vector $\mathbf{e}^\dagger(\mathbf{r},\omega_0)$, which is a solution to the equation

$$\int d\mathbf{r}'\mathbf{e}^\dagger(\mathbf{r}',\omega_0)\cdot\mathbf{g}(\mathbf{r}',\mathbf{r},\omega_0,\alpha_{cr})=0.$$

When $0<\alpha/\alpha_{cr}-1\ll 1$ and the nonlinear current is sufficiently small, the eigenfunction $\mathbf{e}(\mathbf{r},\omega)$ must be peaked about $\omega=\omega_0$. We can then expand $\mathbf{g}(\mathbf{r},\mathbf{r}',\omega,\alpha)$ about $\omega=\omega_0$ and $\alpha=\alpha_{cr}$. To eliminate the lowest order term, we take a dot product of Eq. (1) with $\mathbf{e}^\dagger(\mathbf{r},\omega_0)$ and integrate over all space. This procedure reduces Eq. (1) to

$$\int d\mathbf{r}d\mathbf{r}'\mathbf{e}^\dagger(\mathbf{r},\omega_0)\cdot[(\omega-\omega_0)\mathbf{g}_\omega(\mathbf{r},\mathbf{r}',\omega_0,\alpha_{cr})+(\alpha-\alpha_{cr})\mathbf{g}_\alpha(\mathbf{r},\mathbf{r}',\omega_0,\alpha_{cr})]\cdot\mathbf{E}(\mathbf{r}',\omega)$$

$$=\int d\mathbf{r}\mathbf{e}^\dagger(\mathbf{r},\omega_0)\cdot\mathbf{J}_{NL}(\mathbf{r},\omega)$$

where a subscript indicates a partial derivative. It is now allowable to use the lowest order expression for $\mathbf{E}(\mathbf{r},\omega)$ in this equation, namely we put

$$\mathbf{E}(\mathbf{r},\omega)=c(\omega)\mathbf{e}(\mathbf{r},\omega_0).$$

The factor $c(\omega)$ represents the Fourier components peaked at $\omega=\omega_0$. The real electric field of the mode is

$$\mathbf{E}(\mathbf{r},t)=C(t)\exp(-i\omega_0 t)\mathbf{e}(\mathbf{r},\omega_0)+\text{c.c.} \tag{2}$$

where $C(t)$ is a slowly varying mode amplitude. Transformation to the time domain gives the following equation for $C(t)$:

$$iG_\omega\frac{dC}{dt}+(\alpha-\alpha_{cr})G_\alpha C=e^{i\omega_0 t}\int d\mathbf{r}\mathbf{e}^\dagger(\mathbf{r},\omega_0)\cdot\mathbf{J}_{NL}(\mathbf{r},t) \tag{3}$$

where

$$G(\omega,\alpha)\equiv\int d\mathbf{r}d\mathbf{r}'\mathbf{e}^\dagger(\mathbf{r},\omega_0)\cdot\mathbf{g}(\mathbf{r},\mathbf{r}',\omega,\alpha)\cdot\mathbf{e}(\mathbf{r},\omega_0)$$

and

$$G_\omega=\int d\mathbf{r}d\mathbf{r}'\mathbf{e}^\dagger(\mathbf{r},\omega_0)\cdot\mathbf{g}_\omega(\mathbf{r},\mathbf{r}',\omega_0,\alpha_{cr})\cdot\mathbf{e}(\mathbf{r},\omega_0)$$

$$G_\alpha = \int d\mathbf{r}d\mathbf{r}'\mathbf{e}^\dagger(\mathbf{r},\omega_0)\cdot\mathbf{g}_\alpha(\mathbf{r},\mathbf{r}',\omega_0,\alpha_{cr})\cdot\mathbf{e}(\mathbf{r},\omega_0).$$

In order to evaluate the nonlinear term in Eq. (3), we first express $\mathbf{J}_{NL}(\mathbf{r},t)$ in terms of the particle distribution function, which gives

$$e^{i\omega_0 t}\int d\mathbf{r}\mathbf{e}^\dagger(\mathbf{r},\omega_0)\cdot\mathbf{J}_{NL}(\mathbf{r},t) = qe^{i\omega_0 t}\int d\Gamma\mathbf{e}^\dagger(\mathbf{r},\omega_0)\cdot\mathbf{v}(\mathbf{r},\mathbf{p})f_{NL}(\mathbf{r},\mathbf{p},t). \tag{4}$$

Here, q is the particle charge, $d\Gamma = d\mathbf{r}d\mathbf{p}$ is the phase space volume element, $\mathbf{v}(\mathbf{r},\mathbf{p})$ is the particle velocity, and $f_{NL}(\mathbf{r},\mathbf{p},t)$ is the nonlinear part of the distribution function.

We now need to find $f_{NL}(\mathbf{r},\mathbf{p},t)$ from the kinetic equation

$$\frac{\partial f}{\partial t} + [H,f] = Stf + Q \tag{5}$$

in which the Hamiltonian H splits into $H = H_0 + H_1$ with H_0 being the nonperturbed Hamiltonian that determines the equilibrium orbits, and H_1 the perturbation from the mode. The right-hand side of Eq. (5) takes into account particle source Q and collision operator, St. We assume the nonperturbed motion described by H_0 to be fully integrable, which allows canonical transformation to action-angle variables. Let I_i with $i = 1, 2, 3$ be the actions and ξ_i be the corresponding canonical angles, so that all physics quantities are periodic functions of ξ_i with the period 2π. Then, the Hamiltonian H can be cast into the form

$$H = H_0(I_1,I_2,I_3) + H_1 \tag{6}$$

with

$$H_1 = 2\,\mathrm{Re}\,C(t)e^{-i\omega_0 t}\sum_{\ell_1,\ell_2,\ell_3} V_{\ell_1,\ell_2,\ell_3}(I_1,I_2,I_3)e^{i\ell_1\xi_1+i\ell_2\xi_2+i\ell_3\xi_3} \tag{7}$$

where ℓ_1, ℓ_2, and ℓ_3 are integers, and $V_{\ell_1,\ell_2,\ell_3}(I_1,I_2,I_3)$ are matrix elements that can be calculated in a standard way, given the mode structure and the nonperturbed particle orbits. We have neglected C^2 and other higher order corrections to H as it can be shown that they produce small terms in the final equation, compared to the terms we will generate.

For nearly resonant particles we can relate H_1 to the perturbed electric field given by Eq. (2). The result is

$$H_1 = 2q\,\mathrm{Re}\left(iC(t)\frac{\mathbf{v}\cdot\mathbf{e}}{\omega_0}\,e^{-i\omega_0 t}\right).$$

With this expression for H_1, we find

$$V_{\ell_1,\ell_2,\ell_3}(I_1,I_2,I_3) = \frac{iq}{\omega_0}\int\frac{d\xi_1 d\xi_2 d\xi_3}{(2\pi)^3}\exp\left[-i(\ell_1\xi_1+\ell_2\xi_2+\ell_3\xi_3)\right]\mathbf{v}\cdot\mathbf{e}.$$

Each term in the perturbed Hamiltonian represents a resonance that can be treated separately if the resonances do not overlap, which we assume here to be the case. For the motion dominated by a single resonance, the summation sign can be dropped in Eq. (7). One can then choose a new set of action-angle variables so that one of the new angles is $\xi = \ell_1\xi_1 + \ell_2\xi_2 + \ell_3\xi_3$, and I is the corresponding action. The Hamiltonian then reduces to the one-dimensional form

$$H = H_0(I) + 2\,\mathrm{Re}\,C(t)e^{-i\omega_0 t}V(I)\exp(i\xi) \tag{8}$$

where the remaining variables, not shown here, are suppressed as they can be treated as parameters in the new Hamiltonian. The resonance action I_r is determined by the equation

$$\Omega(I_r) = \omega_0$$

where $\Omega(I) \equiv \frac{\partial H_0}{\partial I} = \ell_1\frac{\partial H_0}{\partial I_1} + \ell_2\frac{\partial H_0}{\partial I_2} + \ell_3\frac{\partial H_0}{\partial I_3}$. The collisionless motion of a resonant particle satisfies the pendulum equation

$$\frac{d^2\xi}{dt^2} + \omega_b^2\sin(\xi - \omega_0 t - \xi_0) = 0 \tag{9}$$

where

$$\omega_b \equiv |2CV(I_r)\partial\Omega(I_r)/\partial I_r|^{1/2}$$

is the nonlinear bounce frequency of the particle (when C is time independent) and ξ_0 is a constant phase.

Near the resonance, the kinetic equation reads

$$\frac{\partial f}{\partial t} + \Omega(I)\,\frac{\partial f}{\partial \xi} - 2\,\mathrm{Re}[iC(t)V(I_r)\,\exp(i\xi - i\omega_0 t)]\frac{\partial f}{\partial I} = Stf + Q. \tag{10}$$

In this equation, we have neglected the term $\frac{\partial H_1}{\partial I}\frac{\partial f}{\partial \xi}$, which is indeed a justified approximation: this term is small compared to the last term on the left-hand side of Eq. (10) because the perturbed distribution function of the resonant particles has a steeper gradient in I than the perturbed Hamiltonian. For the same reason, we treat the matrix element and $\partial\Omega/\partial I$ as constants evaluated at $I = I_r$ when we solve Eq. (10) for the resonant particles.

We will consider two different descriptions of collisions in Eq. (10): a simplified Krook model and a more realistic diffusive model. For the Krook model, we take

$$Stf + Q = -\nu_r(f - F) \tag{11}$$

where F is the equilibrium distribution function with a nearly constant nonzero slope near the resonance, and ν_r is the relaxation rate. The diffusive collisional operator takes the form

$$Stf + Q = \nu_{\mathrm{eff}}^3 \frac{\partial^2}{\partial \Omega^2}(f - F) \tag{12}$$

where F is again the equilibrium distribution. Equation (12) and the expression for ν_{eff}^3 can be consistently derived from a specific Fokker-Planck collision operator with an appropriate orbit averaging procedure developed in Ref. 23. The specific form for ν_{eff}^3 is given in section (c) of the Appendix. Note that only second derivative terms with the perturbed distribution function need to be retained in the collision operator as these are the dominant terms near the resonance where the perturbed distribution is strongly peaked. Equations (11) and (12) lead to similar results if one takes $\nu_r \sim \nu_{\mathrm{eff}}$. The ν-parameter in both equations describes the rate particles decorrelate from resonance when $C(t)$ is sufficiently small.

We explicitly solve Eq. (10) for the Krook model (we shall also present the results for the diffusive model) with the use of a perturbation technique that assumes that either the time

interval is short compared with the characteristic bounce period, $2\pi/\omega_b$, or the collisional relaxation rate is much greater than ω_b. This assumption allows us to seek f in the form of a truncated Fourier series

$$f = F + f_0 + [f_1 \exp(i\xi - i\omega_0 t) + f_2 \exp(2i\xi - 2i\omega_0 t) + \text{c.c.}] \tag{13}$$

where the Fourier coefficients f_0, f_1, and f_2 are functions of t and I. Although the second harmonic generally needs to be included in the calculations of the nonlinear response, it turns out that f_2 does not affect the resulting equation for the mode amplitude. Therefore, we ignore f_2 from the very beginning, a procedure that can be verified in a straightforward way. With this simplification, Eqs. (10) and (11) reduce to

$$\frac{\partial f_1}{\partial t} - i[\omega_0 - \Omega(I)]f_1 + \nu_r f_1 = iC(t)V\frac{\partial}{\partial I}(F + f_0) \tag{14}$$

$$\frac{\partial f_0}{\partial t} + \nu_r f_0 = iC(t)V\frac{\partial f_1^*}{\partial I} - iC^*(t)V^*\frac{\partial f_1}{\partial I}. \tag{15}$$

We integrate Eqs. (14), and (15) iteratively taking into account that $F \gg f_1 \gg f_0$ and assuming zero initial values for f_1 and f_0. We first neglect f_0 on the right-handside of Eq. (14) and find f_{1L}, the part of f_1, linear in C:

$$f_{1L} = i\int_0^t d\tau e^{-\nu_r(t-\tau)}V\frac{\partial F}{\partial I}C(\tau)e^{i(\omega_0-\Omega)(t-\tau)}.$$

Next, we use f_{1L} instead of f_1 in Eq. (15) to find f_0. We then substitute f_0 into Eq. (14) and calculate f_{1NL}, the part of f_1 cubic in C. For $\omega_0 t \gg 1$, the dominant contribution to f_{1NL} comes from the terms in which the differential operator $\frac{\partial}{\partial I}$ acts on the exponential functions in f_{1L} and f_0. The final leading order contribution to f_{1NL} has the form

$$f_{1NL} = -i\int_0^t d\tau\int_0^\tau d\tau_1\int_0^{\tau_1} d\tau_2(\tau_1-\tau_2)^2 e^{-\nu_r(t-\tau_2)}V|V|^2\left(\frac{\partial\Omega}{\partial I}\right)^2\frac{\partial F}{\partial I}$$

$$\cdot\left[C(\tau)C(\tau_1)C^*(\tau_2)e^{i(\omega_0-\Omega)(t-\tau-\tau_1+\tau_2)} + C(\tau)C^*(\tau_1)C(\tau_2)e^{i(\omega_0-\Omega)(t-\tau+\tau_1-\tau_2)}\right]. \tag{16}$$

The nonlinear term on the right-hand side of Eq. (3) is a functional of f_{1NL}. The evaluation of this term involves an integration over phase space, including integration over I, or alternatively, over $\Omega(I)$. As a function of Ω, the integrand is a product of a smooth function, which can be treated as constant near the resonance, and the exponential functions in f_{1NL}. Once integrated over Ω, the exponential functions generate two δ-functions: $\delta(t-\tau-\tau_1+\tau_2)$ and $\delta(t-\tau+\tau_1-\tau_2)$, of which only the first one falls into the time domain of Eq. (16). This observation leads to the following structure of Eq. (3):

$$iG_\omega \frac{dC}{dt} + (\alpha - \alpha_{cr})G_\alpha C =$$

$$K \int_0^t d\tau \int_0^\tau d\tau_1 \int_0^{\tau_1} d\tau_2 \delta(t-\tau-\tau_1+\tau_2)(\tau_1-\tau_2)^2 e^{-\nu_r(t-\tau_2)} C(\tau)C(\tau_1)C^*(\tau_2) \qquad (17)$$

where

$$K = 2\pi\omega_0 \int d\Gamma \delta(\omega_0 - \Omega) V^\dagger V |V|^2 \left(\frac{\partial\Omega}{\partial I}\right)^2 \frac{\partial F}{\partial I}, \qquad (18)$$

$$V^\dagger = -\frac{iq}{\omega_0} \int \frac{d\xi_1 d\xi_2 d\xi_3}{(2\pi)^3} \mathbf{e}^\dagger \cdot \mathbf{v} \exp(i\xi), \qquad (19)$$

and for simplicity we have taken ν_r independent of phase space position.

When Eqs. (17)–(19) are applied to specific problems, transformation from I to more natural variables can be useful. For example, natural transformation of the operator $\frac{\partial}{\partial I}$ for a tokamak is given in section (a) of the Appendix.

It is convenient to measure time in Eq. (17) in the units of γ^{-1}, where γ is the linear instability growth rate. In addition, we introduce a new unknown function

$$A = aC\exp(ibt)$$

where a and b are real constants whose values are such that Eq. (17) takes the standard form

$$\frac{dA}{dt} = A - e^{i\phi} \int_0^{t/2} \tau^2 d\tau \int_0^{t-2\tau} d\tau_1 e^{(-2\nu\tau - \nu\tau_1)} A(t-\tau)A(t-\tau-\tau_1)A^*(t-2\tau-\tau_1) \qquad (20)$$

where $\nu = \nu_r/\gamma$, and ϕ is a constant angle defined by the relation

$$e^{i\phi} \equiv iK|G_\omega|/(|K|G_\omega).$$

A similar derivation can be carried out with the diffusive collision operator (12). The resulting dimensionless equation has the form

$$\frac{dA}{dt} = A - e^{i\phi} \int_0^{t/2} \tau^2 d\tau \int_0^{t-2\tau} d\tau_1 e^{-\nu^3\tau^2(2\tau/3+\tau_1)} A(t-\tau)A(t-\tau-\tau_1)A^*(t-2\tau-\tau_1) \qquad (21)$$

where $\nu = \nu_{\text{eff}}/\gamma$.

In the perturbative case, the matrix $\mathbf{g}$ in Eq. (1) is nearly Hermitian, which gives $\mathbf{e}^\dagger = \mathbf{e}^*$ and $V^\dagger = V^*$. The factor K is real in this case. One can also show that G_ω is purely imaginary for any Hermitian matrix $\mathbf{g}$ and that $\mathrm{Im}\, G_\omega$ has the same sign as the mode energy. We thus conclude that the value of ϕ can only be 0 or π in the perturbative case. Note that $\phi = 0$ applies for the frequently studied situation of a positive energy wave with negative dissipation from resonant particles.

The absolute value of the dimensionless amplitude A in these Eqs. (20), (21) measures the square of the nonlinear bounce frequency ω_b, namely

$$\omega_b^2 \approx \gamma_L^2 \left(\frac{\alpha - \alpha_{cr}}{\alpha_{cr}}\right)^{5/2} |A|. \qquad (22)$$

with γ_L the growth rate when $1 - \alpha_{cr}/\alpha \approx 1$. It should also be noted that the presence of a small parameter $\left(\frac{\alpha-\alpha_{cr}}{\alpha_{cr}}\right)^{5/2}$ in Eq. (22) is the basis of justifying the neglect of higher order nonlinear terms in this derivation, as long as $|A| \ll [\alpha_{cr}/(\alpha - \alpha_{cr})]^{5/2}$. Further discussion of the applicability range of Eqs. (20) and (21) is given in section (b) of the Appendix.

III. Steady-State Saturation, Limit Cycle, Explosion

Equation (20) is of the form derived in Ref. 2, except for the additional phase factor $e^{i\phi}$ and the complex conjugate appearing in the nonlinear term. In the limit of large t, Eq. (20)

has a periodic solution with constant amplitude:

$$A = \frac{2\nu^2}{(\cos\phi)^{1/2}} \exp(-it\tan\phi), \tag{23}$$

a generalization of the steady state solution found in Ref. 2 for $\phi = 0$. A similar solution can be readily obtained for Eq. (21):

$$A = \frac{\nu^2}{\left(\cos\phi \int_0^\infty dz \exp(-2z^3/3)\right)^{1/2}} \exp(-it\tan\phi). \tag{24}$$

Solutions (23) and (24) imply that the nonlinear term has a stabilizing effect; this requires $\cos\phi$ to be positive. For a system with a negative value of $\cos\phi$, weak nonlinearity can never balance the linear drive in an unstable system, and this always leads to a hard nonlinear scenario where the mode grows to a large amplitude regardless of closeness to the instability threshold. Note that $\cos\phi > 0$ is a necessary but not a sufficient condition for the mode to saturate at a low level. A hard scenario is possible even when $\cos\phi > 0$. In this case, however, it requires sufficiently low collisionality (see below). We also note that the hard regime can arise in a linearly stable system if the initial perturbation is sufficiently large.

We now address the question of stability for the constant amplitude solutions (23) and (24). In order to make the analysis more compact, we use the transformation

$$A = a(t)\exp(-it\tan\phi) \tag{25}$$

and also combine Eqs. (20) and (21) into

$$\frac{da}{dt} = (1 + i\tan\phi)a - \frac{e^{i\phi}}{\nu^2}\int_0^\infty d\tau \int_0^\infty d\tau_1 Q(\nu\tau, \nu\tau_1)a(t-\tau)a(t-\tau-)a^*(t-2\tau-\tau_1) \tag{26}$$

with $Q(x,y) = x^2e^{-2x-y}$ for Eq. (20) and $Q(x,y) = x^2e^{-x^2(2x/3+y)}$ for Eq. (21). We have extended the integration limits in Eq. (26) to infinity, reflecting the limit of large t. We now linearize Eq. (26) about the steady state $\alpha = \alpha_0 = \text{const}$ with

$$|a_0^2| = \nu^4 \left[\cos\phi \int_0^\infty dx \int_0^\infty Q(x,y)dy\right]^{-1} \tag{27}$$

and look for a solution of the form

$$a = a_0 + \delta a_1 \exp(\nu\lambda t) + \delta a_2 \exp(\nu\lambda^* t) \tag{28}$$

with λ an eigenvalue. The solvability condition for the ensuing linear equations for δa_1 and δa_1^* yields the dispersion relation

$$\lambda^2\nu^2\cos^2\phi - 2\lambda\nu\cos^2\phi Q_1 + Q_1^2 = Q_2^2 \tag{29}$$

where

$$Q_1(\lambda) = \left[\int_0^\infty dx \int_0^\infty Q(x,y)dy\right]^{-1} \int_0^\infty dx \int_0^\infty dy Q(x,y)[1 - \exp(-\lambda x) - \exp(-\lambda x - \lambda y)]$$

$$Q_2(\lambda) = \left[\int_0^\infty dx \int_0^\infty Q(x,y)dy\right]^{-1} \int_0^\infty dx \int_0^\infty dy Q(x,y)\exp(-2\lambda x - \lambda y)$$

For large values of $\nu(\nu \gg 1)$ all roots of Eq. (29) have $\mathrm{Re}\,\lambda < 0$, while if ν is sufficiently small unstable roots are found. The critical value of ν (for each of the two relaxation models) at which the first unstable root appears is shown in Fig. 1 as a function of ϕ. When the steady state nonlinear solution is unstable, the mode cannot converge to the steady level. What develops instead when ν is close to the critical value, is a limit cycle of the type discussed in Ref. 2. Examples of such behavior are shown in Fig. 2. As ν goes deeper into the unstable range, bifurcations destroy periodicity of the cycle but the mode amplitude can still be limited in this regime (see Fig. 2). Further, at even smaller values of ν, the mode develops an explosive singularity, evolving into a hard nonlinear regime that runs out of the applicability range of Eqs. (20) or (21).

Examples of the explosive solutions were found in Ref. 2. Here, we present similar, though somewhat different analytic solutions of the Eqs. (20), (21). As in the analysis in Ref. 2, we set $\nu = 0$ and neglect the linear drive, looking for a solution that evolves very fast and becomes singular at a finite time t_0. In this limit, there is no difference between Eqs. (20)

and (21). We look for a solution of the form

$$A(t) = g[\chi(t)](t_0 - t)^{-5/2} \tag{30}$$

where $g[\chi]$ is a periodic function of $\chi \equiv \ln(t_0 - t)$. One readily observes that this structure of A allows a common time factorization and then we can reduce Eqs. (20) and (21) to

$$e^{-i\phi}\left(\frac{5}{2}g - \frac{dg}{d\chi}\right) = \int_0^\infty d\xi \int_0^\infty d\eta U(\xi,\eta) g[\chi+\ln(1+\xi)] g[\chi+\ln(1+\xi+\eta)] g^*[\chi+\ln(1+2\xi+\eta)] \tag{31}$$

with

$$U(\xi,\eta) = \frac{\xi^2}{(1+\xi)^{5/2}(1+\xi+\eta)^{5/2}(1+2\xi+\eta)^{5/2}}.$$

We now observe that

$$g(\chi) = \rho \exp(i\sigma\chi) = \rho \exp[i\sigma \ln(t_0 - t)]. \tag{32}$$

is an exact solution to Eq. (31) if the constants ρ and σ, with σ real, satisfy the complex relation

$$e^{-i\phi}\left(\frac{5}{2} - i\sigma\right) = |\rho|^2 \int_0^\infty d\xi \int_0^\infty d\eta U(\xi,\eta) \exp\left\{i\sigma \ln[(1+\xi)(1+\xi+\eta)/(1+2\xi+\eta)]\right\}$$

that can also be rewritten as

$$e^{-i\phi}\left(\frac{5}{2} - i\sigma\right) = |\rho|^2 \int_0^\infty dz\ F(z) \exp(i\sigma z) \tag{33}$$

with

$$F(z) = e^{-7z/2} \int_0^1 \frac{s^3 ds}{[1+s(1-e^{-z})^{1/2}]^4 [1+s(1-e^{-z})^{-1/2}]^2}.$$

Thus, in order for σ to be real, we require

$$\frac{\sigma\cos\phi + \frac{5}{2}\sin\phi}{\sigma\sin\phi - \frac{5}{2}\cos\phi} = \frac{\int_0^\infty dz\, F(z)\sin(\sigma z)}{\int_0^\infty dz F(z)\cos(\sigma z)}. \tag{34}$$

A plot of σ vs. ϕ for two roots of Eq. (34) is shown in Fig. 3. Note that these roots are related by symmetry: if $\sigma(\phi)$ is a root of Eq. (34), then $\sigma(-\phi) = -\sigma(\phi)$ is also a root.

An interesting feature of the presented explosive solution is that it describes the effect of chirping: it follows from Eq. (32) that the mode frequency increases with time if σ is a positive number and vice versa [decreases if σ is negative]. When the kinetic response is non-perturbative, the frequency shift in the explosive regime can reach a substantial fraction of the mode's initial frequency before solution (30) breaks due to higher nonlinearities. An example of such a behavior is shown in Fig. 4.

When $\phi = 0$, the numerical solution to Eq. (20) for small values of ν seems to follow the symmetric explosive solution described in Ref. 2 . However, for $|\phi| \gtrsim \pi/8$, the numerical solutions is closer to the chirping explosive solution [given by Eqs. (30) and (32)] where the smaller absolute value of σ, plotted in Fig. 3, is taken.

It should be noted that the oscillations of the mode amplitude described by Eqs. (30)–(32) are not directly due to particle trapping (indeed, particle trapping would only occur when the explosive solution is beyond its range of validity). The qualitative explanation for these oscillations is that when the slope of the particle distribution function decreases nonlinearly at the location of the original resonance, steeper slopes build up on both sides of the resonance next to it. In the symmetric case ($\phi = 0$) discussed in Ref. 2, the mode frequency splits into two sidebands that tend to grow faster than the original mode. Hence, an explosive overall growth of the amplitude with the oscillations at the beat frequency that increases as the sidebands move apart. This process continues until the mode traps resonant particles and forms the plateau on the distribution function near the resonance. The corresponding peak amplitude of the mode is unrelated to the closeness to the instability threshold. For the bump-on-tail problem, this peak amplitude can be estimated from the condition $\omega_b \approx \gamma_L$ where γ_L is the instability growth rate without the background damping. This is a much higher level than the underestimated value $\omega_b \approx \gamma$ presented in Ref. 2. For those instabilities

that have $\gamma = \omega$ far above the threshold, ω_b can grow up to $\omega_b \approx \omega$. This makes the applicability range for the explosive solution much broader than originally expected.

IV. Applications

A. Toroidal Alfvén Eigenmodes in TFTR

Regimes in which the Toroidal Alfvén Eigenmode instability is at threshold have been found in TFTR when ICRF minority-ion heating produces fast tail ions which are sometimes augmented by alpha particles in DT discharges.[24] Many features observed in this experiment are consistent with inferences that can be drawn from our nonlinear theory.

One example, shown in Fig. 5a, is the situation when the TAE signals decrease in amplitude but still persist when the applied RF power is shut off. This feature illustrates the role of collisional relaxation of resonant fast particles in maintaining a steady level of the TAE signal. Prior to $t = 3.805\,\mathrm{s}$ (indicated by arrow in Fig. 5a), the RF power is on, and fast ions are produced at a heating rate ν_h that is roughly proportional to the applied power. The ICRF heating is a diffusive process that renews the distribtution function of the resonant particles at a relatively quick rate $\nu_{\mathrm{eff}} \approx (\nu_h \omega_{\mathrm{TAE}}^2)^{1/3}$, with ω_{TAE} the TAE frequency. When the heating is turned off, the principal relaxation mechanism that persists is collisional pitch angle scattering of resonant ions, with $\nu_s \approx 0.1\nu_h$, so that ν_{eff} decreases to roughly half of the RF-on value. This leads to a lower level of quasi-stationary oscillations, as seen after $t = 3.805\,\mathrm{s}$. Figure 5b presents a model for the two quasi-stationary levels seen in the experiment, a numerical solution of Eq. (21) (generalized to the case of time dependent ν) which shows a decrease in saturation level when ν is abruptly reduced by 1/2. The TAE signal in Fig. 5a eventually disappears after RF turn-off. The reason is that the fast ions slow down. As a result, their instability drive becomes weaker than the dissipative effects from the background plasma. This appears to occur on a time scale about 1/10th the slowing-down

time, presumably because the original fast-ion distribution is only slightly above marginal stability.

A second example is the time evolution of a single mode that grows from the onset of instability to a saturated state as shown by the dots in Fig. 6. This figure also shows a theoretical fit to the experimental data for the system that goes through the instability threshold. In the simulation, the mode growth rate, γ, is taken to vary linearly in time from $\gamma = 0$ to $\gamma = 0.1\gamma_L$ where γ_L is the energetic particle growth rate in the absence of dissipation. From the fitting, we infer that the ratio of perturbed to equilibrium magnetic field is roughly 10^{-5}, and the RF heating time is 0.2 s; results that are consistent with the experiment.[24] This correlation indicates that the collisional relaxation process can indeed be an important ingredient in the long time evolution of a weak TAE instability.

B. Fishbones

A fishbone is an internal rigid "kink" displacement of the plasma column in a tokamak.[17,18] It develops within the magnetic surface on which the safety factor q equals unity, with $q < 1$ in the interior. If the perturbed MHD potential energy is positive, continuum damping precludes the ideal kink mode from existing in absence of energetic particles. However, with a large enough energetic particle pressure confined within the $q = 1$ surface, kinetic drive from the precessional drift resonance can overcome continuum damping and make the kink mode unstable.

To illustrate the link between our theoretical model and the evolution of the fishbone instability, we neglect such additional factors as plasma resistivity, thermal ion diamagnetic frequency effects, finite ion Larmor radius effects and fluid-type nonlinearities. In reality, these factors are not always negligible and can play an important role in the interpretation of the experimental results. To simplify the discussion even further, we consider the energetic particles to be deeply trapped in the equilibrium mirror field of the torus and to have thin

"banana" orbits. The distribution of these particles is taken to be Maxwellian in energy and to have a flat density profile that abruptly goes to zero at some radius inside the $q = 1$ surface. With this idealization, the dispersion relation derived in Ref. 25 can be schematically written in the form

$$G(\omega, \alpha, \delta) = -1 - i\frac{\delta}{\omega} + i\alpha \int_0^\infty \frac{dx x \exp(-x)}{\omega - x} = 0 \tag{35}$$

where ω is the normalized frequency relative to typical precession drift frequency, the positive parameter δ is proportional to the perturbed MHD energy, and α is the normalized pressure of the energetic particles.

At marginal stability, Eq. (35) yields ω real, which translates into the following relations for δ and α:

$$\alpha = \frac{1}{\pi\omega} e^\omega; \qquad \delta = \frac{1}{\pi} e^\omega \, \mathrm{Re} \int_0^\infty \frac{dx x \exp(-x)}{\omega - x}. \tag{36}$$

One can infer that both δ and α are monotonic functions of ω in the range where $\delta > 0$. Taken together, relations (36) determine α_{cr} for the onset of instability as a function of the parameter δ. The plot of α_{cr} vs. δ shown in Fig. 7 indicates that the system is stable at a sufficiently large perturbed MHD energy and can be destabilized by increasing energetic particle pressure.

A separate calculation shows that the value of K determined by Eq. (18) is nearly real and positive in our idealized model of the fishbones. Therefore, the phase ϕ, that appears in the nonlinear Eqs. (20) and (21), is $\arg(i\partial G^*/\partial\omega)$ or equivalently

$$\phi = \arg\left[\frac{1}{\omega}\frac{\partial}{\partial\omega}\omega \, \mathrm{Re} \int_0^\infty \frac{dx x \exp(-x)}{\omega - x} - i\pi(\omega - 1)e^{-\omega}\right].$$

A plot of ϕ vs. δ is shown in Fig. 7. We see that $-\pi/2 < \phi < 0$, for $0 < \delta < \delta_c$, and that $\phi < -\pi/2$ for $\delta > \delta_c$.

The case $\phi < -\pi/2$ corresponds to a very hard nonlinear response with a destabilization from the cubic nonlinearity. In this case there is no steady nonlinear solution.

The case where $0 > \phi > -\pi/2$, and $\nu \to 0$, is what we conjecture describes fishbone oscillations. It is clear that the mode can arise at a broad range of parameters. The finite ϕ value leads to a downward frequency shift as the mode blows up. This follows from the numerical solutions of Eq. (21), where the mode frequency is observed to decrease as the mode gets larger. A preliminary comparison of the explosive solution with the experimental data[26] on the onset of the fishbone instability reveals a promising correlation between the two (see Fig. 8).

C. Single Bunch Microwave Instability in Circular Accelerators

A microwave instability usually arises when the number of particles in a circulating bunch exceeds a critical value that depends on parameters of the accelerating regime. The mode emerges as a result of interaction of the perturbed beam with the high-frequency impedance of the vacuum chamber. The instability causes "turbulent bunch lengthening" and increases the energy spread of the beam.[22]

Recent observations in the SLC damping ring at SLAC[27] with a new low-impedance vacuum chamber revealed interesting nonlinear regimes of this instability. In some cases, initial exponential growth was found to saturate at a level that remained constant through the accumulation cycle. In other cases, relaxation-type oscillations occurred at the nonlinear stage of the instability. The frequency of the unstable mode tends to be close to the second harmonic of the synchrotron oscillations. Similar effects have been observed in LEP for the oscillations of the bunch length.[28]

A vast literature devoted to this instability is mostly focused on the linear analysis aimed to quantify the instability threshold and the mode structure for a given wake in the accelerator (see e.g. Ref. 29). Recent efforts[30] to address the nonlinear problem rely on sophisticated numerical tools rather than on developing simplified analytical models. The theory presented in this paper adds to a purely numerical approach by offering an analytical

model for the interpretation of the experimental results. Another attempt to treat the problem semi-analytically with an emphasis on the resonant particle response was recently made in Ref. 31.

In order to quantitatively compare our theory with experiment, detailed computations for specific experimental conditions are needed to determine the values of the parameters in the nonlinear equations. However, even without the calculation of the exact values of the parameters, we can compare the patterns of the signal measured in the experiments with the solutions of Eq. (21). Note that the diffusive collisional operator (12) used in the derivation of Eq. (21) is a relevant model for the quantum diffusion of beam particles in phase space due to synchrotron radiation. In our comparison, we only pay attention to qualitative features of the signal, such as growth, oscillation and saturation.

The signal presented in Fig. 5 of Ref. 27 demonstrates the mode saturation at a steady level after the initial growth. The time scale of the transition is comparable with the synchrotron damping time. This signal looks very similar to the solution of Eq. (21) shown in Fig. 2 for $\nu = 6.69$. In another case (see Fig. 4 of Ref. 27), decreasing oscillations of the mode amplitude are observed. This response can be compared with the plot in Fig. 2 for $\nu = 2.71$. In unpublished work by B. Podobedov and R. Siemann, purely periodic behavior of the mode was found, which resembles the limit cycle shown in Fig. 2 for $\nu = 2.03$. The period of the cycle tends to agree with the measurements, although more quantitative work is needed to verify preliminary interpretations.

Acknowledgments

We are appreciative of the useful discussions with J. Candy and M. Mauel. We would like to thank J. Strachan for providing data for Fig. 8.

This work is supported by the U.S. Department of Energy, Contract No. De-FG03-96ER-54346.

Appendix: Technical Details

a. Operator $\partial/\partial I$ in a symmetric torus

For the quiding center motion in a toroidally symmetric magnetic field, the operator $\partial/\partial I$ can be expressed in terms of the three conserved quantities in the nonperturbed field: the particle energy E, the canonical toroidal angular momentum P_ϕ, and the magnetic moment μ. One can readily establish that

$$\partial/\partial I = \ell_1 \partial/\partial I_1 + \ell_2 \partial/\partial I_2 + \ell_3 \partial/\partial I_3.$$

It can also be shown that it is always allowable to take $I_2 = P_\phi$ and $I_3 = \mu mc/q$; here q is the particle charge. The particle energy E as a function of I_1, I_2 and I_3 is the Hamiltonian of the system. We now choose I_1 to be the action for the poloidal motion, so that the quantities $\omega_1 \equiv \partial E/\partial I_1$, $\omega_2 \equiv \partial E/\partial I_2$ and $\omega_3 \equiv \partial E/\partial I_3$ are the frequencies of the poloidal, toroidal and gyromotion, respectively. We can then rewrite the operator $\partial/\partial I$ in the form

$$\partial/\partial I = (\ell_1\omega_1 + \ell_2\omega_2 + \ell_3\omega_3)\partial/\partial E + \ell_2 \partial/\partial I_2 + \ell_3 \partial/\partial I_3.$$

At the resonance, the sum $\ell_1\omega_1 + \ell_2\omega_2 + \ell_3\omega_3$ equals the mode frequency ω. In addition, ℓ_3 must be taken zero for the low-frequency modes, and ℓ_2 is nothing else than the toroidal mode number n. Hence, we find

$$\partial/\partial I = \omega \partial/\partial E + n\partial/\partial P_\phi = \omega \left.\frac{\partial}{\partial E}\right|_{P'_\phi} = n \left.\frac{\partial}{\partial P_\phi}\right|_{E'}$$

with $P'_\phi = P_\phi - nE/\omega$ and $E' = E - \omega P_\phi/n$.

b. Validity limit of cubic integral equation and explosive solution

It is clear from Eq. (9) that the particle motion can be described perturbatively for short enough time scales, satisfying the condition

$$\int_0^t \omega_b dt \ll 1.$$

With collisions present, the time of validity of perturbation theory can be indefinitely long if the decorrelation time τ_c, which is $1/\nu_{\text{eff}}$ or $1/\nu_r$ depending on description of collisions, is less than ω_b^{-1}. Hence, a perturbative treatment is expected to be applicable if

$$\min\left(\int_0^t \omega_b dt; \omega_b \tau_c\right) \ll 1. \tag{A-1}$$

The explicit evaluation of the next (fifth) order nonlinear terms in Eq. (17) shows that those terms are indeed smaller than the cubic term when condition (A-1) is satisfied.

Condition (A-1) sets the limit on ω_b for which the explosive solution is valid. For the explosive solution, the dC/dt term in Eq. (17) equals the nonlinear term with $\nu_r = 0$. This relation gives the following estimate:

$$\frac{1}{C}\frac{dC}{dt} \approx \gamma_L \left(\int_0^t \omega_b dt\right)^4 \ll \gamma_L$$

where γ_L is the instability growth rate far above the threshold (at $\alpha \approx 2\alpha_{cr}$). We then find that the breakdown occurs when

$$\frac{1}{C}\frac{dC}{dt} \approx \gamma_L,$$

which determines the characteristic time scale near the singularity: $\Delta t \approx 1/\gamma_L$. The corresponding limit for ω_b is thus, $\omega_b \approx 1/\Delta t \approx \gamma_L$.

c. Form of ν_{eff}

Suppose the Fokker-Planck operator is of the form

$$St \equiv \frac{\partial}{\partial \mathbf{v}} \cdot \mathbf{D} \cdot \frac{\partial}{\partial \mathbf{v}},$$

where $\frac{\partial}{\partial \mathbf{v}}$ is a velocity space derivative with the spatial position $\mathbf{r}$ fixed, and $\mathbf{D}$ a dyadic describing velocity space diffusion. The distribution function, f, is in general a function of $I(\Omega), \xi$ and two additional action variables, but only the derivative with respect to I is large near the resonance. Hence, the dominant part of the collisional term is

$$Stf = \nu_{\text{eff}}^3 \frac{\partial^2 f}{\partial \Omega^2}$$

with

$$\nu_{\text{eff}}^3 = \overline{\frac{\partial I}{\partial \mathbf{v}} \cdot \mathbf{D} \cdot \frac{\partial I}{\partial \mathbf{v}}} \left(\frac{\partial \Omega}{\partial I} \right)^2 ,$$

where the bar denotes bounce average over the nonperturbed orbit.

Using the result of section (a) of this Appendix we can take $I = P_\phi / n$ at constant E'. Then we find

$$\nu_{\text{eff}}^3 = \overline{\frac{\partial P_\phi}{\partial \mathbf{v}} \cdot D \frac{\partial P_\phi}{\partial \mathbf{v}}} \left(\left. \frac{\partial \Omega}{\partial P_\phi} \right|_{E'} \right)^2 .$$

References

1. Ira B. Bernstein, S.K. Trehen, and M.P.H. Weenink, Nucl. Fusion **4**, 61 (1964).

2. H.L. Berk, B.N. Breizman, and M. Pekker, Phys. Rev. Lett. **76**, 1256 (1996).

3. W.E. Drummond and D. Pines, Nucl. Fusion Suppl, Pt. 3, 1049 (1962).

4. A.A. Vedenov, E.P. Velikhov, and R.Z. Sagdeev, Nucl. Fusion Suppl., Pt. 2, 465 (1962).

5. R.K. Mazitov, Zh. Prikl. Mekh. Techn. Fiz. **1**, 27 (1965).

6. T. O'Neil, Phys. Fluids **8**, 2255 (1965).

7. M.B. Levin, M.G. Lyubarsky, I.N. Onishchenko, V.D. Shapiro, V.I. Shevchenko, Sov. Phys. JETP **35**, 898 (1972); See also National Technical Information Service Order No. AD 730123 (B.C. Fried, C.S. Liu, R.W. Means, and R.Z. Sagdeev, "Nonlinear evolution and saturation of unstable electrostatic unstable wave," Report No. PPG-93, University of California, Los Angeles, 1971). Copies may be ordered from the National Technical Information Service, Springfield, VA, 22161.

8. H.L. Berk, B.N. Breizman, and H. Ye, Phys. Rev. Lett. **68**, 3563 (1992).

9. H.L. Berk, B.N. Breizman, and M. Pekker, in *Physics of High Energy Particles in Toroidal Systems* AIP Conf. Proc. 311, edited by T. Tajima and M. Okamoto (American Institute of Physics, New York, 1994).

10. G.Y. Fu and W. Park, Phys. Rev. Lett. **74**, 1594 (1995).

11. Y. Todo, T. Sato, K. Watanabe, T.H. Watanabe, and R. Horiuchi, Phys. Plasmas **2**, 2711 (1995).

12. H.L. Berk, B.N. Breizman, and M. Pekker, Phys. Plasmas **2**, 3007 (1995).

13. Y. Wu, R.B. White, Y. Chen, and M.N. Rosenbluth, Phys. Plasmas **2**, 4555 (1995).

14. O. Penrose, Phys. Fluids **3**, 258 (1960).

15. A. Simon and M.N. Rosenbluth, Phys. Fluids **19**, 1567 (1976).

16. John David Crawford, Phys. Plasmas **2**, 97 (1995).

17. K. McGuire, R. Goldston, M. Bell, M. Bitter, K. Bol, K. Brau, D. Buchenauer, T. Crowley, S. Davis, F. Fylla, H. Eubank, H. Fishman, R. Fonck, B. Grek, R. Grimm, R. Hawryluk, H. Hsuan, R. Hulse, R. Izzo, R. Kaita, S. Kaye, H. Kugel, D. Johnson, J. Manickam, D. Manos, D. Mansfield, E. Mazzucato, R. McCann, D. McCune, D. Monticello, R. Motley, D. Mueller, K. Oasa, M. Okabayashi, K. Owens, W. Park, M. Reusch, N. Sauthoff, G. Schmidt, S. Sesnic, J. Strachan, C. Surko, R. Slusher, H. Takahashi, F. Tenney, P. Thomas, H. Towner, J. Valley, and R.B. White, Phys. Rev. Lett. **50**, 891 (1983).

18. L. Chen, R.B. White, and M.N. Rosenbluth, Phys. Rev. Lett. **52**, 1122 (1984).

19. W.W. Heidbrink, Plasma Phys. Contr. Fusion **37**, 937 (1995).

20. L. Chen and F. Zonca, Phys. Plasmas **3**, 323 (1996).

21. H.P. Warren, M.E. Mauel, D. Brennan, and S. Taromina, Phys. Plasmas **3**, 2143 (1996).

22. A.W. Chao, "Physics of Collective Beam Instabilities in High Energy Accelerators." Wiley, New York, 1993.

23. S.T. Belyaev and G.I. Budker, "Boltzmann's equation for electron gas in which collisions are infrequent ," in Plasma Physics and the Problem of Controlled Thermonuclear Reactions, edited by M.A. Leontovich (Pergamon Press, London, 1959), Vol. 2, p.431.

24. K.L. Wong, R. Majeski, M. Petrov, J.H. Rogers, G. Schilling, J.R. Wilson, H.L. Berk, B.N. Breizman, M. Pekker, and H.V. Wong, IFSR #753, July, 1996; submitted to Phys. Plasmas.

25. F. Porcelli, R. Stankiewicz, W. Kerner, and H.L. Berk, Phys. Plasmas **1**, 470 (1994).

26. J. D. Strachan, B. Grek, W. Heidbrink, D Johnson, S.M. Kaye, H.W. Kugel, B. Le Blank, K. Mc Guire, Nucl. Fusion **25**, 863 (1985).

27. K. Bane *et al.*, "High-Intensity Bunch Instability Behavior in the New SLC Damping Ring Vacuum Chamber," Proceedings of the 1995 Particle Accelerator Conference on High-Energy Accelerators, Dallas, Texas, May (1995) (IEEE), 1996), **5**, 3109.

28. D. Brandt, K. Cornelis and A. Hofman, "Experimental Observations of Instabilities in the Frequency Domain at LEP," CERN SL/92-15, (1992).

29. K. Oide, "A Mechanism of Longitudinal Single-Bunch Instability in Storage Rings," KEK Report 94-138, 1994); M. D'yachkov and R. Baartman, Particle Accelerators **50**, 105 (1995).

30. R. Baartman and M. D'yachkov, "Simulations of Sawtooth Instability," Proceedings of the 1995 Particle Accelerator Conference on High-Energy Accelerators, Dallas, Texas, May 1995) (IEEE, 1996), **5**, 3119; K.L.F. Bane and K. Oide, "Simulations of the Longitudinal Instability in the New SLC Damping Rings," Proceedings of the 1995 Particle Accelerator Conference on High-Energy Accelerators, Dallas, Texas, May 1995), (IEEE, 1996), **5**, 3105.

31. S.A. Heifets, Phys. Rev. E **54**, 2889 (1996).

FIGURE CAPTIONS

FIG. 1. Stability boundaries for the steady state nonlinear solution. These curves plot the value of ν_{cr} vs. ϕ with the dotted curve for the Krook collisional model and the solid curve for the diffusive collisional model. $\nu < \nu_{cr}$ corresponds to instability of the steady state.

FIG. 2. Transition from steady state saturation to the explosive nonlinear regime as ν decreases. Plots of the absolute value of the normalized amlitude, $|A|$, vs. normalized time t for the diffusive case with $\phi = 0$.

FIG. 3. Nonlinear eigenvalues $\sigma(\phi)$ for the explosive solution.

FIG. 4. Explosive solution of nonlinear integral equation for $\phi = -\pi/8$. The oscillatory curve shows the normalized amplitude proportional to $\mathrm{Re}[A(t)\exp(-i\omega_0 t)]$, and the monotonic curve shows the frequency shifting down in time.

FIG. 5. Decrease and persistence of Alfvén signal. Figure (a) shows the TFTR signal after turnoff of RF power. Figure (b) shows the replication of this effect achieved with the nonlinear mode equation by an abrupt decrease of ν_{eff}.

FIG. 6. Comparison of theoretical prediction of mode evolution to saturation with TFTR data (dots).

FIG. 7. Stability boundary $\alpha_{cr}(\delta)$ and phase factor $\phi(\delta)$ for the fishbone model. The mode is linearly unstable at $\alpha > \alpha_{cr}$. For $|\phi| < \pi/2$ ($\delta < \delta_c$), both the soft and the hard nonlinear regimes are possible, depending on collisionality. For $|\phi| > \pi/2$ ($\delta > \delta_c$), weak nonlinearity always leads to the hard regime above the linear threshold.

FIG. 8. Fit of fishbone onset with the explosive chirping solution (open circles show the experimental data from Ref. 26). Note a frequency downshift and a faster than exponential growth of the mode amplitude, which is consistent with the theoretical explosive scenario for $-\pi/2 < \phi < 0$.

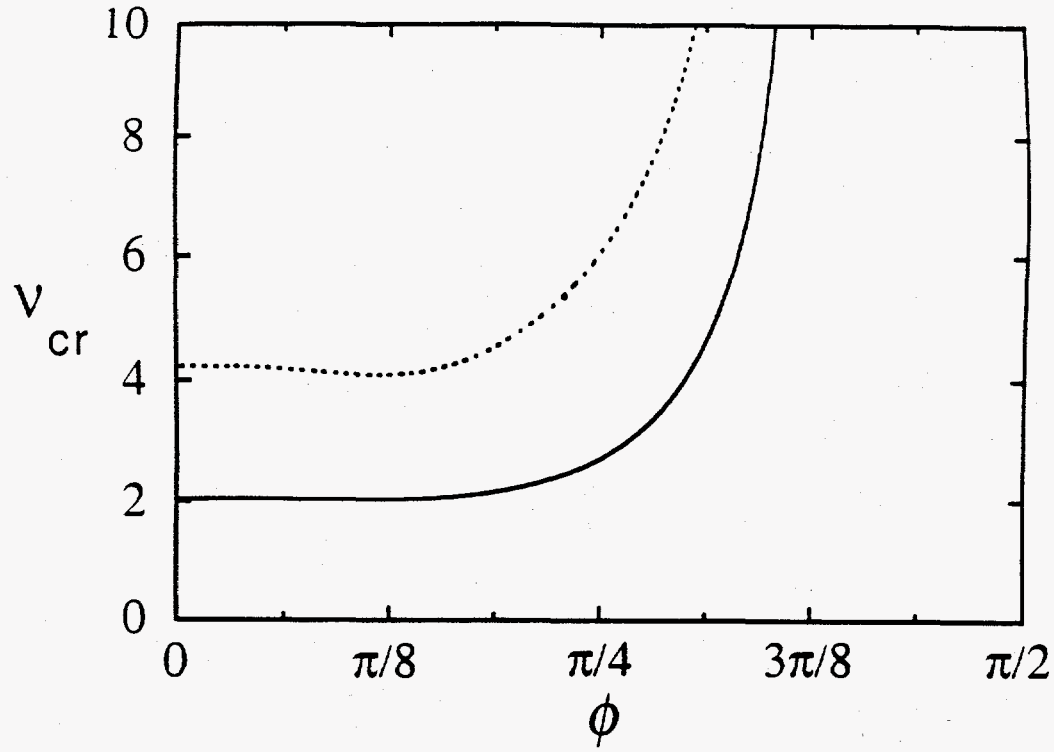

Fig. 1

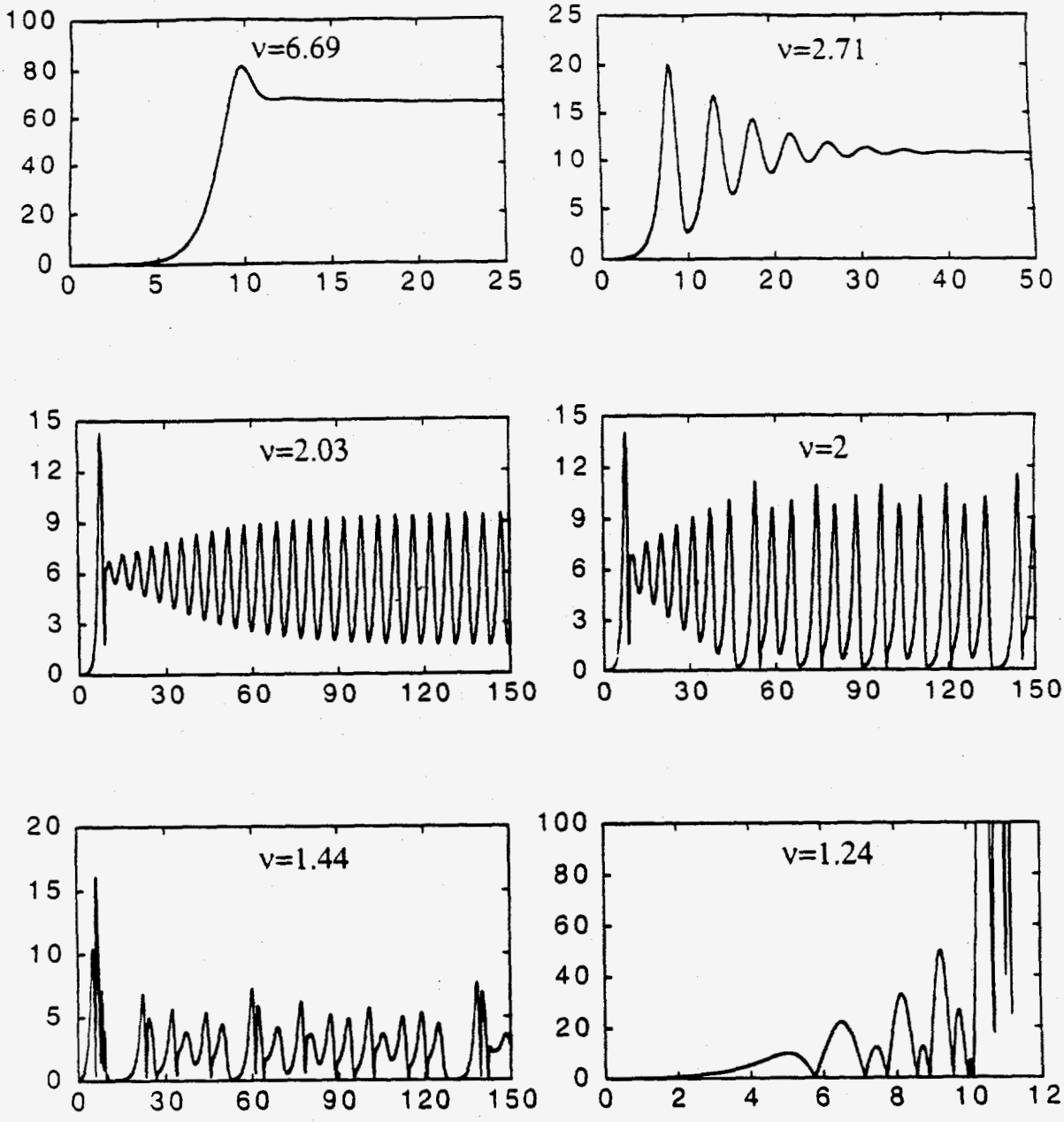

Fig. 2

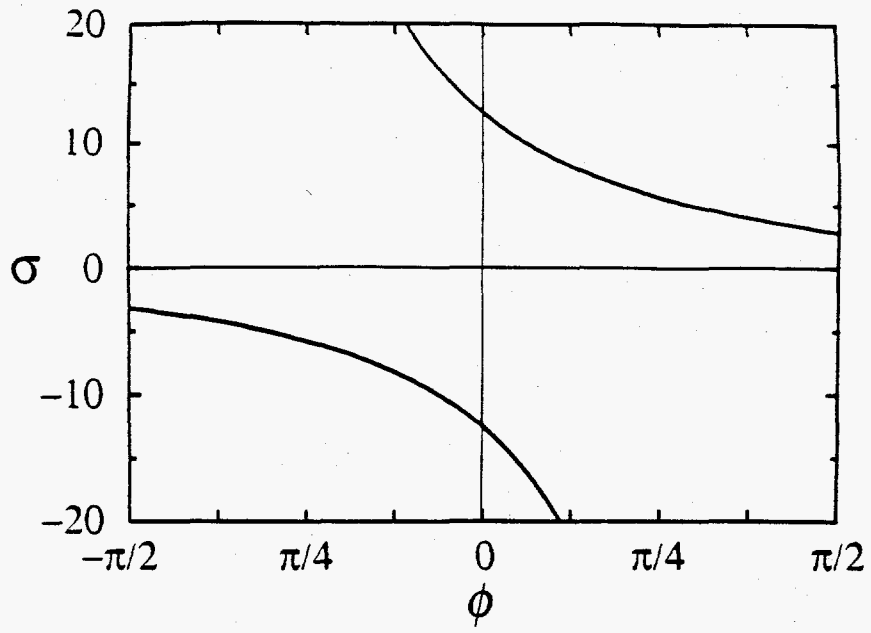
20
10
σ 0
−10
−20
−π/2
π/4
0
π/4
π/2
φ

Fig. 3

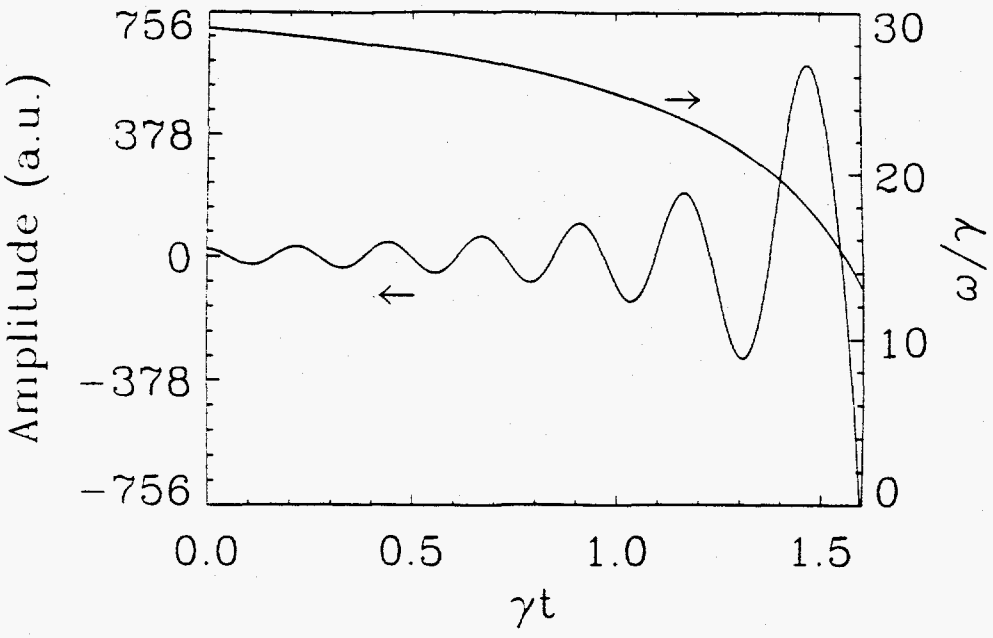
756
378
0
−378
−756
Amplitude (a.u.)
30
20
10
0
ω/γ
0.0
0.5
1.0
1.5
γt

Fig. 4

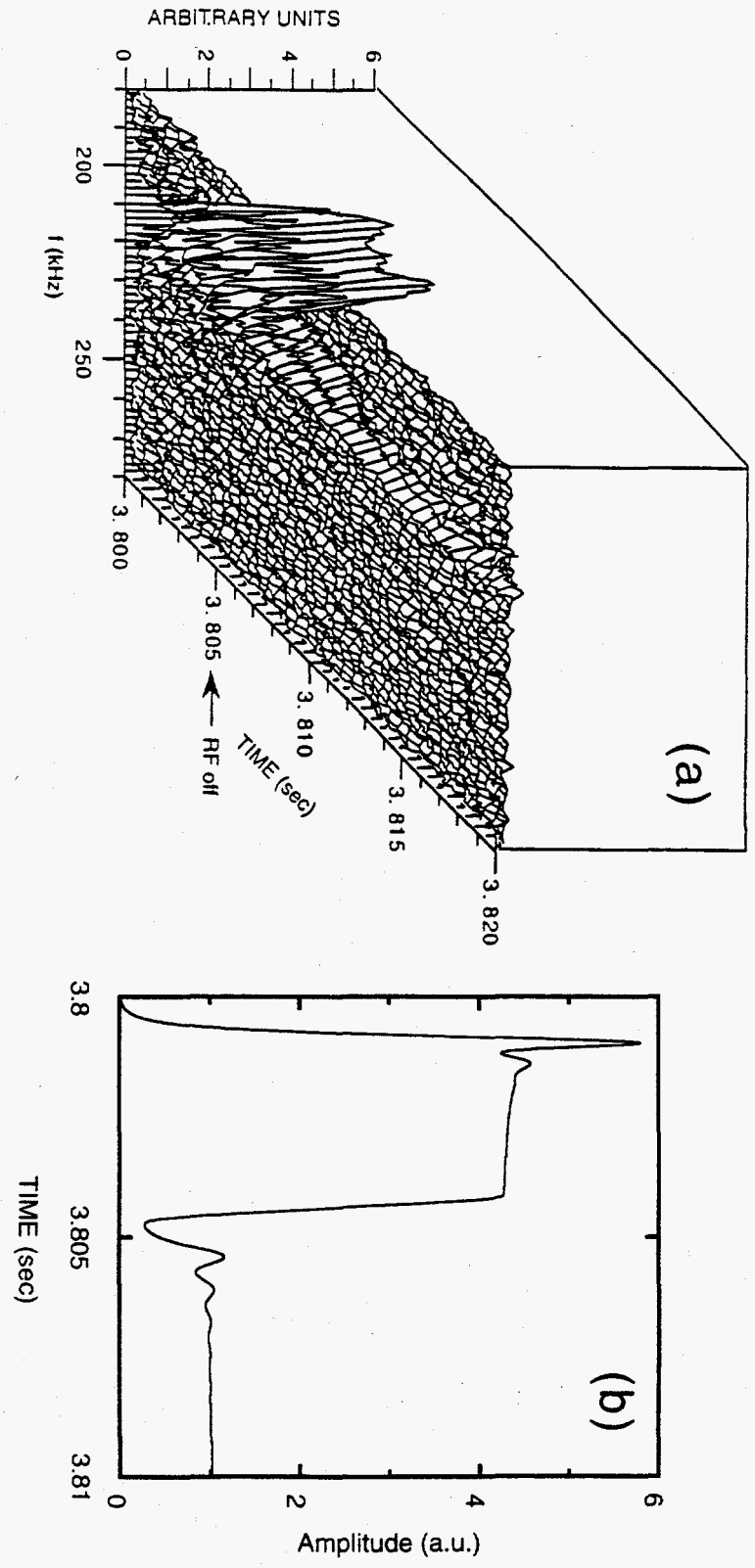
ARBITRARY UNITS
0
2
4
6
200
250
f (kHz)
3. 800
3. 805
3. 810
3. 815
3. 820
TIME (sec)
RF off
(a)
3.8
3.805
3.81
TIME (sec)
0
2
4
6
Amplitude (a.u.)
(b)

Fig.5

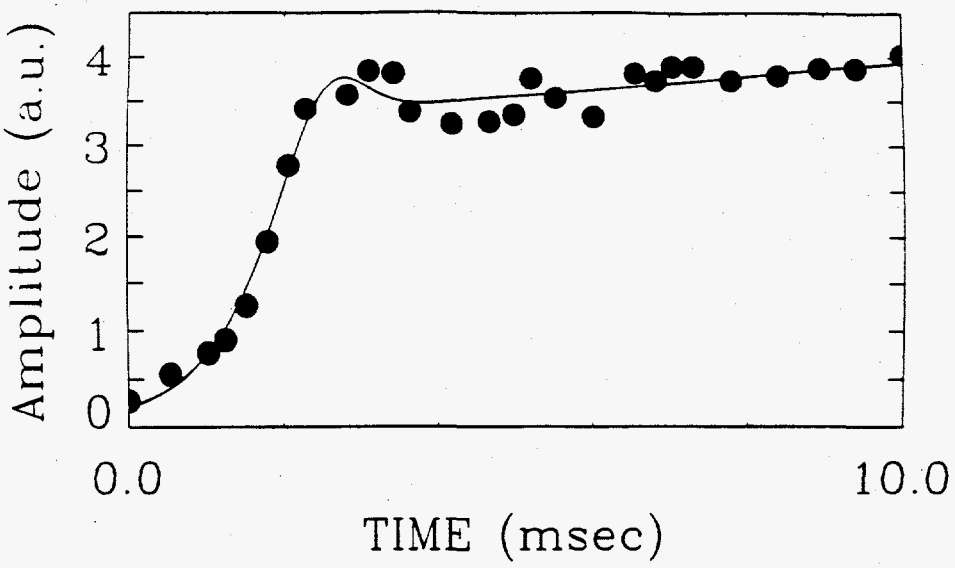
Amplitude (a.u.)
4
3
2
1
0
0.0
10.0
TIME (msec)

Fig. 6

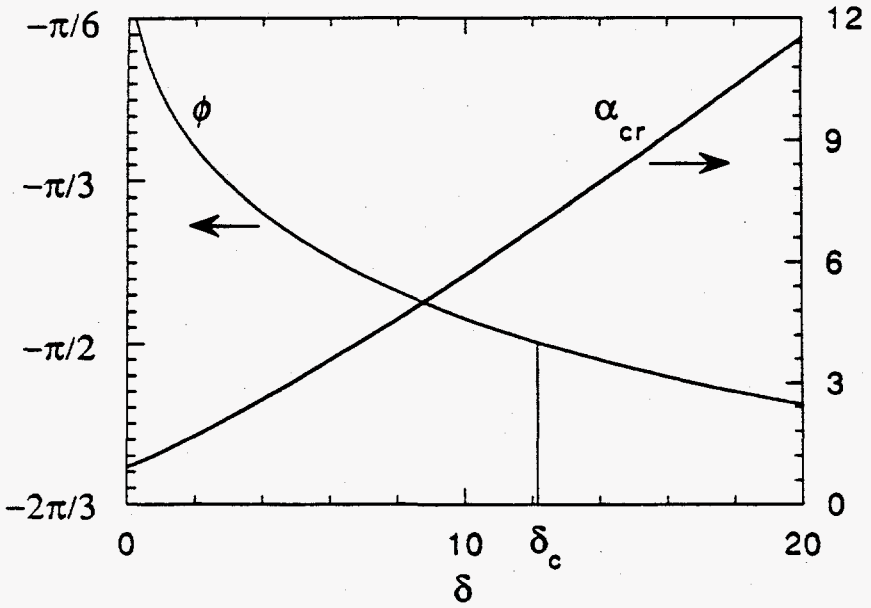
−π/6
−π/3
−π/2
−2π/3
12
9
6
3
0
ϕ
α cr
0
10
δc
20
δ

Fig. 7

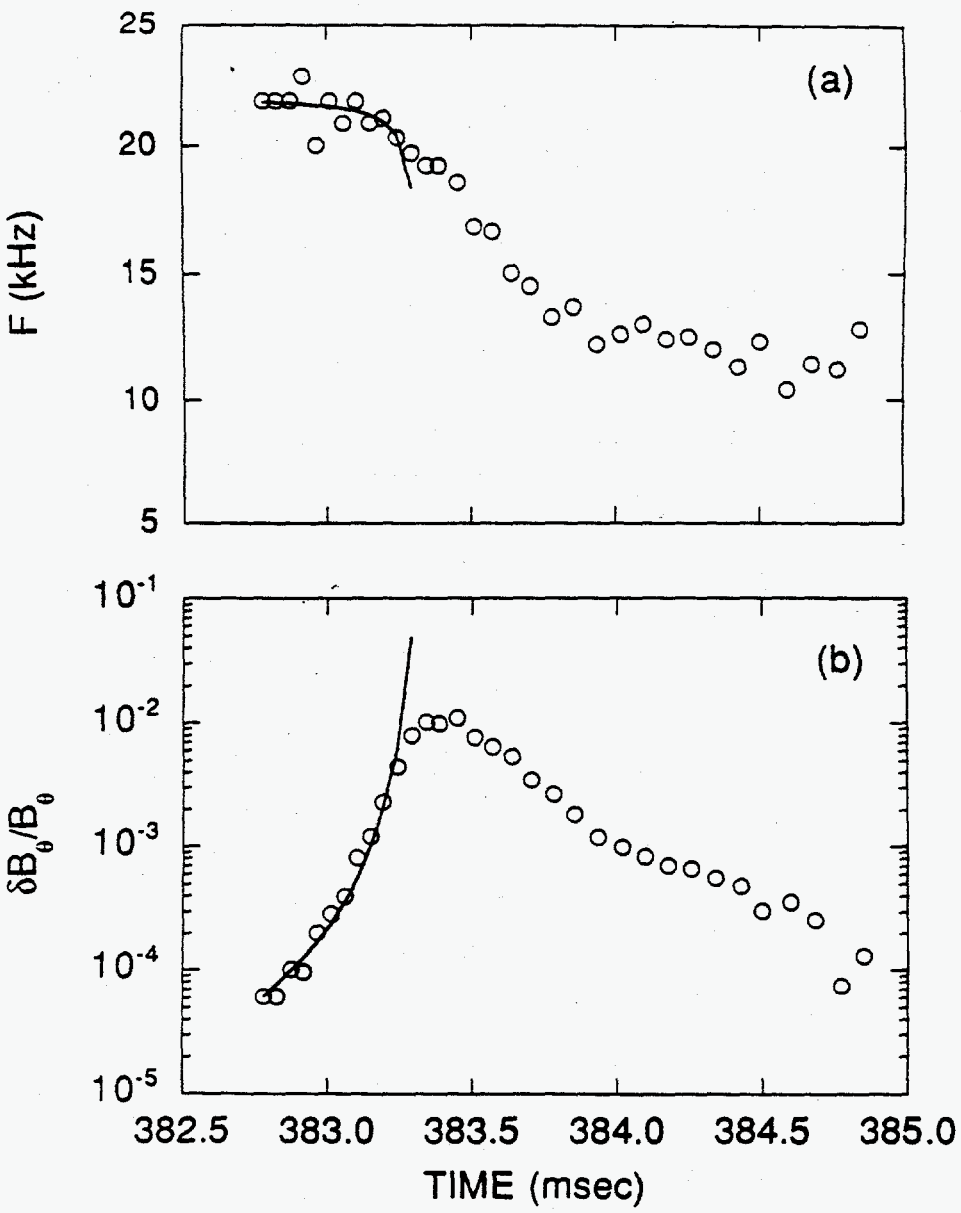
25
20
15
10
5
F (kHz)
(a)
10^{-1}
10^{-2}
10^{-3}
10^{-4}
10^{-5}
$\delta B_\theta / B_\theta$
(b)
382.5
383.0
383.5
384.0
384.5
385.0
TIME (msec)

Fig. 8